Peer-reviewed version available at *Materials* **2020**, *13*, 4089; doi:10.3390/ma13184089

Mixed Oxide-LDHs Materials: Synthesis, Characterization and Efficient Application for Mn^{2+} Removal from Synthetic Wastewater

Cristina Modrogan[1], Simona Căprărescu[2*], Madelene Annette Dăncilă[1*], Oanamari Daniela Orbuleț[1], Eugeniu Vasile[3]

[1] University POLITEHNICA of Bucharest, Faculty of Applied Chemistry and Materials Science, Analitycal Chemistry and Environmental Engineering Department, 1-7 Polizu Str., 011061, Bucharest, Romania, cristina.modrogan@upb.ro; madelene.dancila@upb.ro; oanamari2001@yahoo.com

[2] University POLITEHNICA of Bucharest, Faculty of Applied Chemistry and Materials Science, Inorganic Chemistry, Physical Chemistry and Electrochemistry Department, 1-7 Polizu Str., Bucharest, Romania, simona.caprarescu@upb.ro

[3] Institute of Research and Development "METAV" SA, C.A. Rosetti 31, 020011, Bucharest, Romania; eugeniuvasile@yahoo.com

* Corresponding authors: simona.caprarescu@upb.ro (S.C.); madelene.dancila@upb.ro (A.M.D.)
Tel.: +40214023820 (S.C.)

Abstract: In this study, Mg-Al and Mg-Al-Ni - layered double hydroxides (LDHs) were successfully synthesized for efficient removal of Mn^{2+} from synthetically wastewater. LDH adsorbents (Mg-Al and Mg-Ni-Al) were prepared by co-precipitation method. The formation of the layered double hydroxide, the adsorption of manganese on both LDH (Mg-Al and Mg-Ni-Al) were observed by XRD, SEM and EDX analysis. The various parameters such as the effect of shaking time, initial Mn^{2+} concentration, temperature were controlled and optimized to removal of Mn^{2+} from synthetic wastewater. The kinetics and adsorption isotherms for Mn^{2+} removal from wastewater were studied in batch mode. At temperatures of 10 °C and 20 °C the adsorption equilibrium was reached after 24 h. Adsorption isotherms of Mn^{2+} are well fitted by Langmuir and Freundlich isotherm equation. The adsorption capacity of Mn^{2+} from synthetic wastewater of 80.607 mg/kg was obtained for (Mg-Al-Ni)-LDH. It is found that the adsorption kinetics is best described by the pseudo-second order model. These results prove that LDHs can be considered as a potential material for adsorption of Mn^{2+} from wastewater.

Keywords: mixed oxide-LDHs; manganese; wastewater; adsorption kinetics

1. Introduction

The pollution of water bodies by metals has received increasing public attention due to the importance of metals in industrial processes and their potential toxicity towards humans and in the aquatic environment [1]. In the earth's crust the manganese is frequently associated with iron. The main minerals are: pyrolusite (MnO_2), rhodocrosite ($MnCO_3$), hausmanite (Mn_3O_4), braunite (Mn_2O_3). Manganese oxides can be reduced with coal in furnaces at high temperatures or in electric furnaces. Pure manganese can be obtained by aluminothermy, electrolysis of a concentrated solution of $MnSO_4$ or by sodium dislocation of MnF_2 or $MnCl_2$. [1-3].

Peer-reviewed version available at Materials 2020, 13, 4089; doi:10.3390/ma13184089

The sources of manganese pollution are: siderurgy, being an alloying element with other metals such as: iron, nickel, copper, aluminum; manufacture of dry batteries, glass and ceramics industry, chemical industry, paint industry. Waste waters from industries, mainly the steel manufacturing industry (about 95%), are the main sources of manganese pollution along with the ores processing and exploitation [2].

In organism's manganese is an essential trace element, its function being related to the metabolism of oxygen. The daily dose in humans is 5 - 10 mg. High doses of ingested manganese can cause local affections (burns of the digestive tract, vomiting, glottic edema, digestive bleeding) and general affections (liver, respiratory and cardiovascular disorders). The respiratory tract damage may occur during inhalation in the case of occupational exposures to iron and manganese processing, in the production of alloys, mining, welding and working with agrochemicals products. Symptoms of neurological appear in chronic intoxication and develops slowly, only after years of exposure. It appears headache, asthenia, drowsiness, changes in gait "went of cock" or irreversible effects such as: Parkinson's syndrome, dysgraphia, dysarthria, psychic impairment. From US statistics, a population between 500,000 and 1500,000 people is diagnosed with Parkinson's disease, and doctors are considering a possible exposure to manganese [2]. In drinking water, the concentration of manganese should not exceed 0.1 mg/L. The legislation has established a maximum concentration of manganese in effluent of 1.0 mg/L [3].

Manganese has high solubility under both acid and neutral conditions, which is why it is considered a difficult element to remove from aqueous media. [4]. For the removal of manganese, the most used methods are precipitation processes with carbonates, hydroxides or oxidative precipitation. Reagents such as NaOH or Na_2CO_3, have low selectivity in the case of Mn^{2+}, therefore it is not recommended in the processes of treatment of effluents with low manganese content. [5]. Oxidation of Mn^{2+} to Mn^{4+} can be most easily done with air or O_2 when manganese dioxide is formed, but the reaction has a slow speed. Other oxidation agents used in this process are: potassium permanganate, hypochlorite or ozone [5], but these oxidations have the disadvantage of high costs and special methods of handling the reagents [6].

Various techniques for treating manganese wastewater have proved to be disadvantageous due to the followings: generate of a secondary pollution, are inefficient in the case of low manganese content and high costs are recorded [7]. Therefore, the researchers focused on discovering cheap, environmentally friendly, simple and efficient manganese removal methods. Such methods use anionic clays (LDH) materials that can be synthesized in the laboratory by simple and economical methods whose size is nano [8-13].

LDH have brucite like structure. Wimonsong *et al.* [8] established that the general formula is $[M^{II}(1-x)M^{III}x(OH)_2]^{x+}$ $[A^{n-}{}_{x/n}, zH_2O]^{x-}$, where M^{II} and M^{III} are divalent, respective trivalent cations occupying octahedral positions of the hydroxide layer. They are very positive loadings. A^{n-} is the anion that compensates for the load (n represent the number of moles of co-intercalated water and M^{III} per formula weight of the compound). LDH is a strong positive material resulting by replacing the divalent cations with the trivalent cations and it is balanced by the presence of A^{n-} anions in the interlayer. These anions can be exchanged with other anions [9, 10]. These materials are characterized by large specific surfaces and high porosity, thermal stability and anion exchange capacity (2-3 mg/g) [11-13].

Peer-reviewed version available at Materials 2020, 13, 4089; doi:10.3390/ma13184089

To understand the structure of these compounds it is necessary to start from the structure of brucite, $Mg(OH)_2$ brucite consists of infinite planes of octahedra of Mg^{2+} ions coordinated with 6 OH^- groups. These sheets are stacked on top of each other and are held together by hydrogen bonding. When Mg^{2+} ions are substituted by a trivalent ion having not too different a radius (such as $A1^{3+}$ for hydmtalcite), a positive charge is generated in the hydroxyl sheet. The positive charge is offset by divalent anions (e.g. CO_3^{2-}) that are found in the interlayer region of the two sheets type Brucite. The main features of LDH structures therefore was determined by the nature of the brucite-like sheet, by the position of anions and water in the interlayer region and by the type of stacking of the brucite-like sheets. The crystallization water will be encountered in the space in the intermediate layer [13]. Water and anion have a random location in the area of intermediate layers. Their free movement occurs when the existing links are broken and other new connections are formed. The oxygen atoms of the water molecules and of the $(CO_3)^{2-}$ groups are distributed approximately closely around the symmeuy axes that pass through the hydroxyl groups (0.56 A apart) of the adjacent brucite-like sheet [14]

It is known that LDH is an active adsorbent, but studies on the effects of different parameters on the efficiency of eliminating Mn^{2+} have not been adequately explored [15].

The study aims to synthesize of LDH (Mg-Al and Mg-Ni-Al) for the removal of Mn^{2+} from synthetically wastewater. Also, in this study was investigate the adsorption equilibrium on these LDHs in terms of thermodynamics and kinetics in different experimental conditions such as: pH, stirring time, initial concentration of Mn^{2+} and competing ions. The structural and morphological properties of the mixed oxide-LDHs were investigated by X-ray diffraction (XRD), scanning electron microscopy (SEM) and Energy Dispersive Spectroscopy (EDX) analysis. The environmentally friendly procedure described for synthesis of mixed oxides-LDS is low cost, uses eco-friendly materials and could potentially be applied on an industrial scale.

2. Materials and Methods

$Mg(NO_3)_2{\cdot}6H_2O$; $Al(NO_3)_3$ $9H_2O$; $Ni(NO_3)_2 \cdot 6H_2O$; Na_2CO_3; NaOH; $MnSO_4$ were purchased from Sigma Aldrich and used without further purification. H_2SO_4 was was supplied by Merck. All reagents used were analytical grade. Distillated water was used in this work.

2.1. Synthesis of the (Mg-Al and Mg-Ni-Al)-LDHs materials

The (Mg-Al and Mg-Ni-Al)-LDHs materials was synthesized by chemical co-precipitation method, at constant pH 8.45 (pH-meter JKI JK-PH009). In order to synthesized the Mg-Al LDH a typical procedure was followed: a stoichiometric amounts of reagents $Mg(NO_3)_2{\cdot}6H_2O$ and $Al(NO_3)_3{\cdot}9H_2O$ were dissolved in distilled water (total concentration 1 M, cationic ratio Mg^{2+}:Al^{3+} was 3:1). The obtained solution was added slowly over a Na_2CO_3 solution ($2{\cdot}10^{-3}$ M), under vigorous stirring (200 rot/min). During the synthesis the pH value was kept constant at 8.45 by adding NaOH solution (0.1 M). After that, the obtained mixture was stirred continuously for 30 minutes, at room temperature (22±1 °C). The precipitate formed was left to mature for 12 h, then filtered, washed with distilled water several times and dried in air at room temperature. The precipitate was calcined using an oven at 750 °C for 8 h. After that the obtained powder was left at room temperature for 8 h, then used for

Peer-reviewed version available at Materials 2020, 13, 4089; doi:10.3390/ma13184089

adsorption of manganese ions. A similar procedure was employed for the synthesis of Mg-Ni-Al LDH, using $Mg(NO_3)_2 \cdot 6H_2$, $Al(NO_3)_3 \cdot 9H_2O$ amd $Ni(NO_3)_2 \cdot 6H_2O$ (total concentration 1 M, cationic ratio Mg^{2+}:Ni^{2+}:Al^{3+} was 2:1:1). The calcination temperature was 750 °C, for 8 h.

A schematic pathway for the obtained LDHs was showed in Fig. 1.

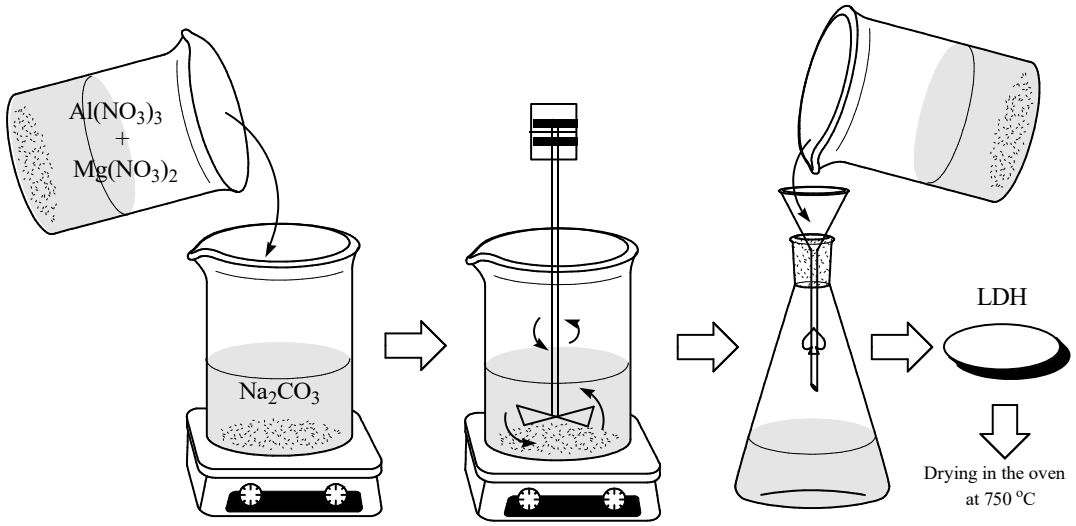

Figure 1. Schematic pathway for obtained LDH

2.2. Characterization of the synthesized materials

The structural properties of the LDHs regarding the adsorption of Mn^{2+} on both Mg-Al-LDH and Mg-NiAl-LDH were observed by Energy Dispersive Spectroscopy (EDX) analysis. The phase composition analysis of the sorbents was performed by X-ray diffraction method using a Shimadzu-6000 diffractometer (2θ Bragg-Brentano geometry, using the CuKα characteristic radiations). The elimination of the CuKβ component was achieved by a Ni filter. The experimental data were digitally collected by the "step by step" scanning method in the 2θ angle interval of 10 ÷ 90 degrees.

The surface morphology of LDHs was performed by Scanning Electron Microscopy (SEM) using a scanning electron microscope Hitachi S2600N.

The textural analysis was performed using Micromeritics ASAP 2020 by adsorption of nitrogen at the liquefaction temperature. The samples were first degassed for 2 hours at 150 °C and 0.1 Pa and then subjected to analysis where they were characterized in terms of the specific surface area, the pore volume and the mean pore size.

The obtained LDHs (see Table 1) were examined before (blank) and after adsorption of Mn^{2+}.

Table 1. Notation of samples before and after adsorption of Mn^{2+}

Samples	Notation
(Mg-Al)-LDH blank	S1
(Mg-Al-Ni)-LDH blank	S2
(Mg-Al)-LDH – Mn^{2+}	S3
(Mg-Al-Ni)-LDH – Mn^{2+}	S4

2.3. Adsorption study of Mn^{2+} used LDH

Peer-reviewed version available at Materials 2020, 13, 4089; doi:10.3390/ma13184089

In order to establish equilibrium conditions for Mn^{2+} removal from synthetical wastewaters were used mixed oxides (Mg-Al and Mg-Al-Ni)-LDHs. Stock solutions that contain Mn^{2+} were prepared by dissolving $MnSO_4$ in deionized water at room temperature (22 ± 2 °C). The working solutions were prepared by diluting the stock solution with deionized water and H_2SO_4 used to adjust the pH to the preset values.

The experimental procedure for the dynamic studies was: 0.3 g mixed oxides (Mg-Al and respectively Mg-Al-Ni)-LDHs, was placed in Berzelius glasses, were added 50 cm^3 $MnSO_4$ solution with various concentrations: 5 mg/L; 15 mg/L; 30 mg/L; 50 mg/L; 100 mg/L. The glasses were coated in order to prevent solution evaporation. The mixed oxides-LDHs was in contact with the solution for 24 hours then filtered using blue ribbon paper and solution was placed in volumetric flask of 50 mL. From the filtrate, 10 cm^3 solution was spectrophotometrically analyzed at λ = 525 nm (Shimatzu 1900 UV-VIS). LDH was used like powder and boring.

The experimental procedure for the kinetic studies was: 0.3 g mixed oxides-LDHs was placed in Berzelius glasses, were added 50 cm^3 $MnSO_4$ solution with concentration of 100 mg/L. The glasses were coated in order to prevent solution evaporation and were stirred (200 rpm) at different times (5, 10, 20, 30, 60, 90 minutes) at 10 °C and 20 °C.

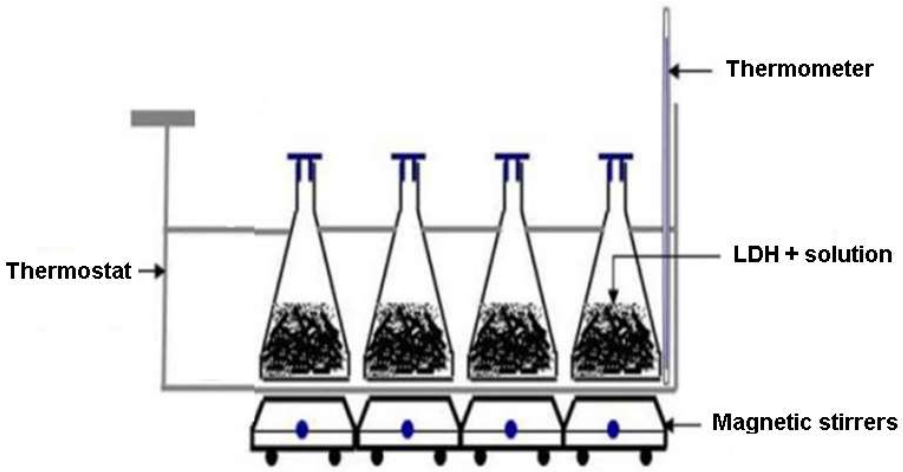

Figure 2. Adsorption study of Mn^{2+} used LDH

Magnetic stirring was realized using a Heidolph Unimax shaker at 300 rpm. At the end of the stirring, the samples were filtered using blue ribbon paper and solution was placed in 50 mL volumetric flask (Figure 2). From the filtrate, 10 cm^3 solution was spectrophotometrically and analyzed at λ = 525 nm. All the experiments were made at pH = 7 (pH-meter JKI JK-PH009, 0 - 14 pH).

2.3.1. Kinetic and thermodynamics study of Mn^{2+}-LDHs

To evaluate the adsorption capacity of LDHs for Mn^{2+}, adsorption isotherm studies were carried out at different temperatures (10 and 20 °C). The experimental data were fitted on the Freundlich and Langmuir models.

The Langmuir model starts from the model of an adsorbent on whose surface are active centers with residual valences. The model hypothesis that covalent bonds are formed between the

Peer-reviewed version available at Materials 2020, 13, 4089; doi:10.3390/ma13184089

surface of the adsorbent and the molecules of the adsorbed component, and there are no interactions between the molecules of the adsorbed component [15].

$$a = \frac{K \cdot C \cdot a_{max}}{1 + K \cdot C} \quad (1)$$

where: K - the equilibrium constant of the adsorption process (mg/L); C – Mn^{2+} concentration in the aqueous phase, at equilibrium (mg/L); a_{max} - maximum adsorption capacity of LDH (mg/kg); a - adsorption capacity of LDH at equilibrium (mg/kg).

Equation (1) is linearized, obtaining the following form [15]:

$$\frac{1}{a} = \frac{1}{K \cdot C \cdot a_{max}} + \frac{1}{a_{max}} \quad (2)$$

In equation (2) the following changes of variable have to be done: $\frac{1}{a} = y$; $\frac{1}{C} = x$ obtaining the equation of a straight line of form: $y_c = A \cdot x + B$

Starting from the equilibrium data obtained experimentally and carrying out the afford mentioned variable changes, the parameters of the straight line are calculated by linear regression.

The Freundlich model starts from the hypothesis of reaching the chemical equilibrium when there is a dynamic exchange between the molecules of the adsorbed phase and those remaining in solution [15]:

$$a = K \cdot C^m \quad (3)$$

where: K, C and a have the same meaning as in equation (1), and m is a constant, in other words another parameter of the Freundlich model.

Equation (3) can be linearized by logarithmation:

$$\ln a = \ln K + m \ln C \quad (4)$$

Noting y = lna and x = lnC, equation (4) can been written:

$$y_c = A \cdot x + B \quad (5)$$

The parameters of the straightline are calculated by linear regression, finally obtaining the parameters of the Freundlich model (K, m).

These equations are widely used, the former being empirical while the second assumes that the maximum adsorption occurs when the surface is covered by the functional groups. Langmuir developed a theoretical equation, considering that a monomolecular adsorption layer occurs on an energetically homogeneous surface, and that there is no interaction between the adsorbed molecules. The Langmuir adsorption isotherm plot (q_e vs. C_e). C_e indicates the applicability of Langmuir adsorption isotherm. The values of q_m and b were calculated from the slope and the intercept of the linear plots C_e/q_e vs. C_e. To predict the adsorption efficiency of the adsorption process, the dimensionless equilibrium parameter was determined by using the following equation (6) [15]:

$$q_e = \frac{q_m \cdot b \cdot C_e}{1 + b \cdot C_e} \quad (6)$$

where: C_e – Mn^{2+} concentration in the aqueous phase, at equilibrium (mg/L); q_e - the adsorbent equilibrium concentration (mg/g); q_m - the adsorbent capacity for a monolayer adsorption (mg/g); b - equilibrium constant [15].

3. Results and discussions

Peer-reviewed version available at Materials 2020, 13, 4089; doi:10.3390/ma13184089

3.1. Characterization of LDH

To further reveal the interaction of Mn^{2+} with LDHs, the XRD analysis was performed. Figure 4 showed the XRD spectra of LDHs before and after Mn^{2+} adsorption.

The mixed oxide LDH had XRD peak patterns different those of from manganese oxide (Fig. 4), which indicates that the LDHs have a different crystal structure from a simple physical mixture of manganese oxides, that is, a homogeneous single phase.

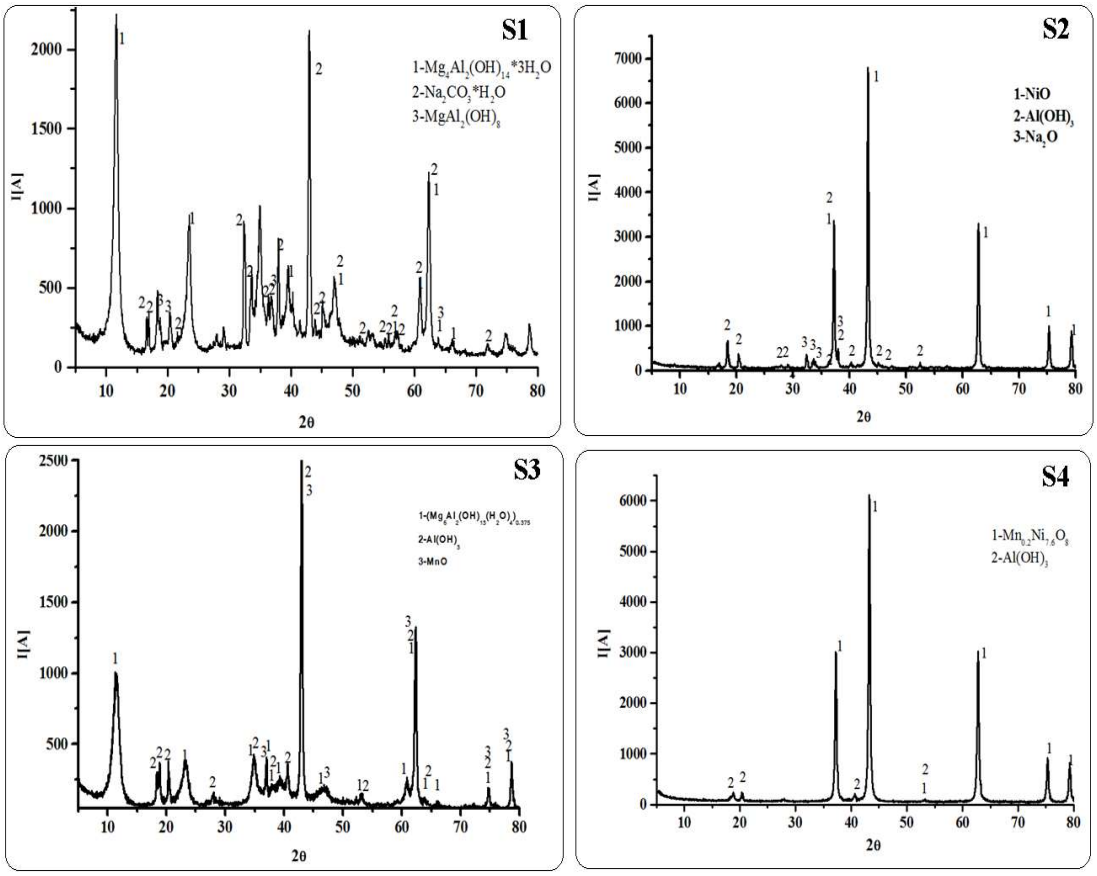

Figure 3. XRD pattern of the LDHs before and after Mn^{2+} adsorption.

The XRD patterns of LDHs before and after Mn^{2+} adsorption (Fig. 3) indicated that the diffraction intensity of peaks decreases and the basal distance increases after reaction, indicating the incorporation of manganese species into the interlayer of the LDHs.

As indicated in the Figure 3, the XRD pattern of the prepared adsorbent before adsorption presented sharp and symmetrical peaks and some high-angle asymmetrical peaks, demonstrating the formation of highly crystalline Mg-Al LDH structure. The phases encountered for the sample S1 are $Na_2CO_3 \cdot H_2O$ - 50% crystallized in the orthorhombic system, $Mg_4Al_2(OH)_{14} \cdot 3\ H_2O$ - 47 % crystallized in the rhombohedral system, and $MgAl_2$ (OH) 8-43% crystallized in the monoclinic system. The phases encountered for the sample S2 are NiO 62 % with cubic crystallization and the sides of 4.18 Å, $Al(OH)_3$ - 40% crystallized in monoclinic system and Na_2O - 33% crystallized in orthorhombic system, no Mg compounds were identified in this analysis. The phases encountered for the sample S3 are MnO - 58 % crystallized in the cubic system, $Al(OH)_3$ – 56 % crystallized in the hexagonal system, is in fact β Al $(OH)_3$ and $(Mg_6Al_2\ (OH) \cdot 18(H_2O)_4)$ 0.375 (hydroxide) double Mg and Al hydrated) - 49% crystallized in rhombohedral system. For the sample S4 are indicated two phases: $Al(OH)_3$ - 25 %

Peer-reviewed version available at Materials 2020, 13, 4089; doi:10.3390/ma13184089

crystallized in monoclinic system and a mixed oxide of Mn and Ni - 75 % crystallized in cubic system [16-20].

The surface morphology of the LDHs before and after Mn^{2+} adsorption was observed by SEM at 5000x magnifications (Figure 4).

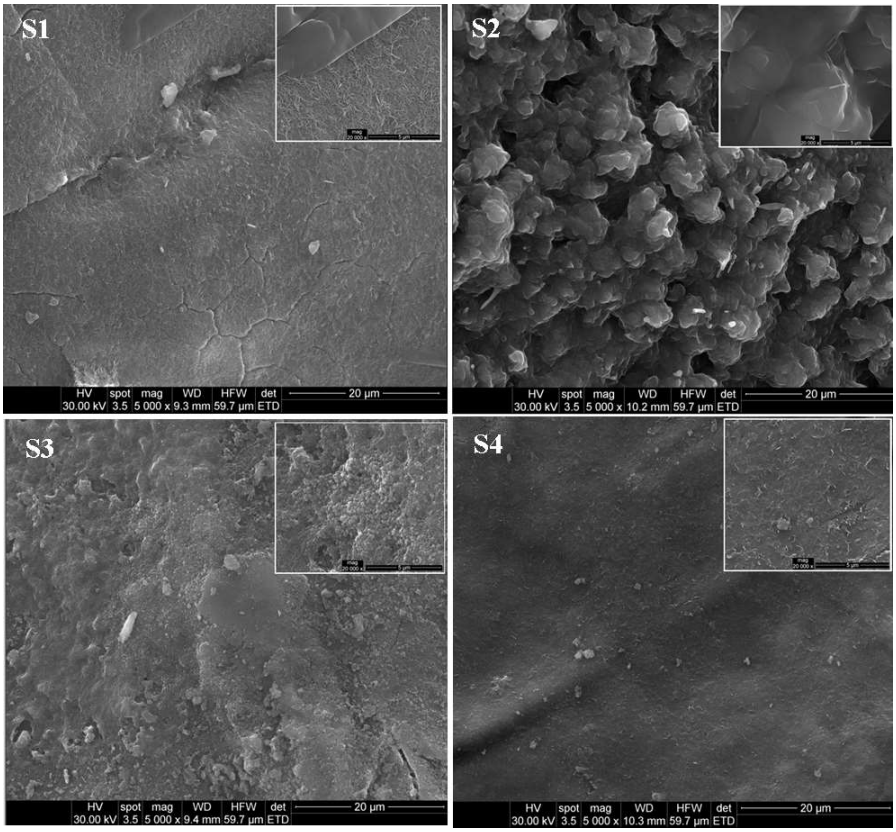

Figure 4. The SEM image for LDHs before and after Mn^{2+} adsorption

It can be observed from the figure 4 that the LDH particles were uniformly shaped sheets, with most of them being hexagonal (gray parts), and the particle size ranged from 200 to 1000 nm in diameter. In addition, several heterogeneous small pores (dark parts) could be noted, which are known to provide larger surface area for contaminant adsorption, thus making the LDH nanoparticles as a well-supported material [19]. Also, Mg-Al-LDH and Mg-Al-Ni-LDH exhibit the agglomerates of compact and non-porous structure. It can be seen that the Mg-Al-LDH had a smaller particle size compared to Mg-Al-Ni-LDH [20].

To further reveal the interaction of manganese with LDHs, the EDX analysis was performed. Figure 5 showed the EDX spectra of LDHs before and after Mn^{2+} adsorption.

Peer-reviewed version available at Materials 2020, 13, 4089; doi:10.3390/ma13184089

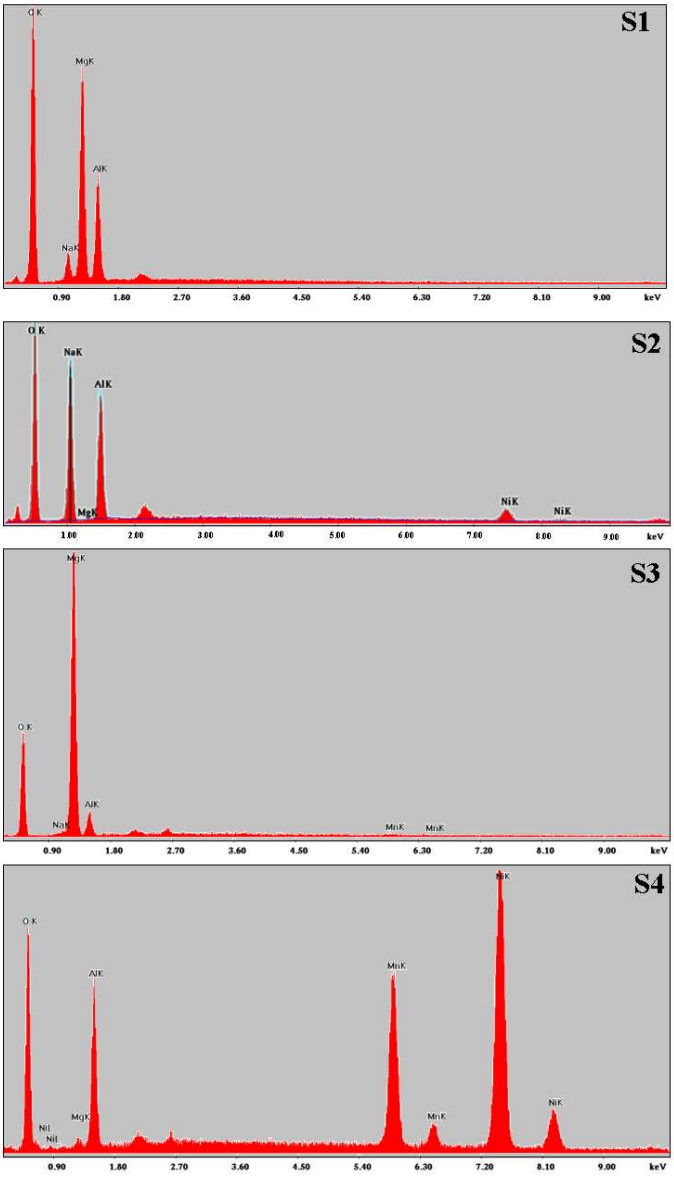

Figure 5. EDX surface analysis of the LDH before and after Mn^{2+} adsorption

In EDX for the sample S1, indicated that the component elements, Mg, Na and Al are highlighted. The calculated quantitative percentages Na-4.52%, Mg-26.50%, Al-16.67% and O - 52.31%, which demonstrates the unevenness of the material. The EDX for the sample S2 showed that the sample has uniformly spread elements, the Mg analysis it is not identified, but the following elements are detected: Na - 30.81%, Al - 22.25% and Ni - 3.97% the rest is O - 42.97%, so in large quantity it is NaO_2. The lack of Mg can be explained by the inclusion of Mg in certain compounds such as aluminum hydroxide and sodium oxide. The compounds are in the form of, sintered crystallites, overlapping. The sample S3 showed a compact surface with small amounts of Mn and the blades are found in the form of very thin sheets and in these small quantities of Mn are recorded. Most of the surface is covered with slats, but compact groups of slats are also observed. Mn retention is uneven, concentrated in different areas. The presence of Mn is detected by the formation of polyhedra, in some areas double pyramids are encountered and the concentration of Mn is greater than 20 %. The retention of Mn is on the interacting surface. From EDX the amount of Mg, Al, Na,

Peer-reviewed version available at Materials 2020, 13, 4089; doi:10.3390/ma13184089

Mn and the rest O was calculated. The elements detected are: O 39.52 %, Na 0.65 %, Mg 50.63 %, Al 8.56 %, Mn 0.63 %. In case of sample S4 it is observed the deposit of a large quantity of Mn, but Na is not detected in the sample. Also, Mg is present, but in small quantity. The presence of Mn is illustrated by the formation of pyramid formations. The presence of Ni favors the retention of Mn, the compound identified by XRD analysis being a mixed oxide of the type $Mn_{0.2}Ni_{7.6}O_8$. The appearance of the sample is quite compact, the very thin blades are arranged, some weights being arranged others in the majority, but also perpendicular to the others. At an increase of 400 000 hours it is observed that on the pyramidal formations there are deposits in the form of crystallites [17-20].

3.2. Kinetics and adsorption isotherms evaluation

The equilibrium adsorption isotherm is important in the adsorption system design. The distribution of manganese between the liquid and the solid phase in equilibrium is expressed by the Freundlich and Langmuir models.

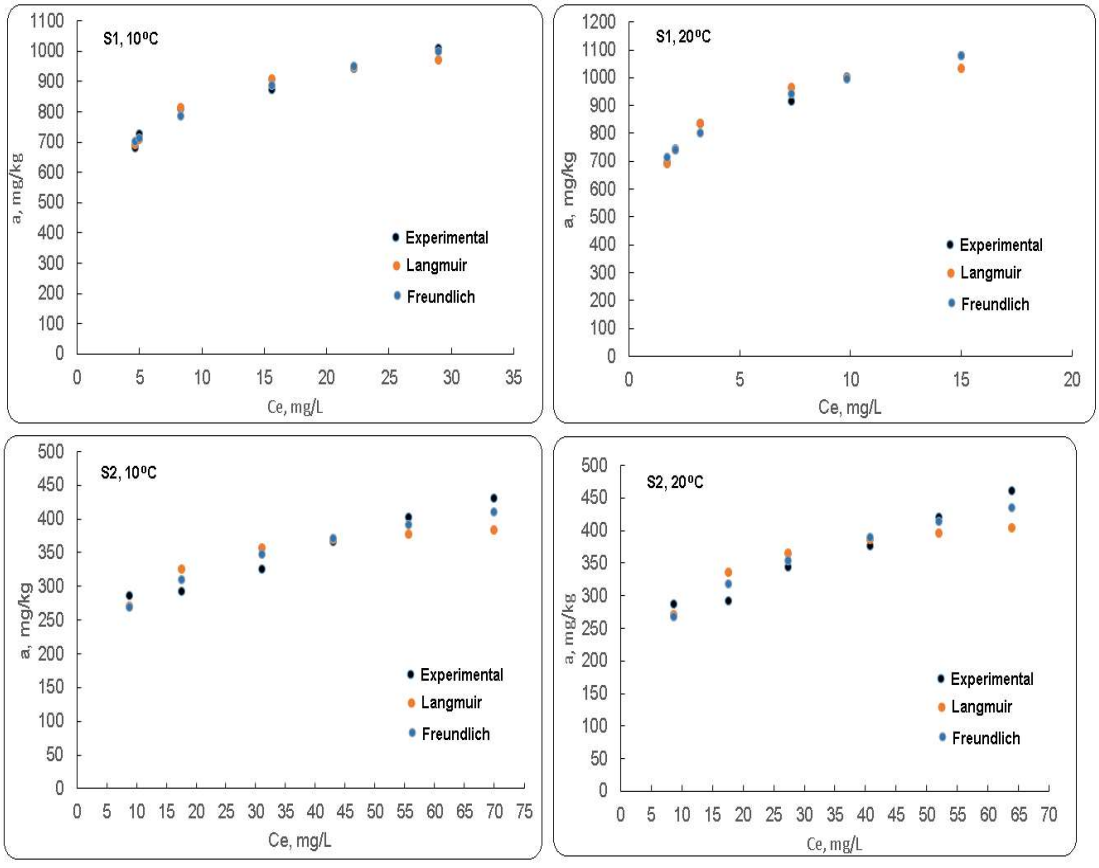

Figure 6. The adsorption curves of Mn^{2+} using Mg-Al-LDH (S1) and Mg-Ni-Al-LDH (S2) at 10 °C and 20 °C

The adsorption isotherm of Mn^{2+} on Mg-Al-LDHs and Mg-Ni-Al-LDHs measured with the initial Mn^{2+} concentration ranging from 5 to 100 mg/L was shown in Figure 6. As we can see, the adsorption capacity of Mn^{2+} increased with increasing the initial Mn^{2+} concentration. The adsorption isotherm parameters from Mg-Al-LDHs and Mg-Ni-Al-LDHs are presented in Table 2. As shown in Table 2, the isotherm data were better fitted into the Langmuir model than the Freundlich model. It can be found that was significant difference between the calculated value (1048.315 mg/kg at 10°C

Peer-reviewed version available at Materials 2020, 13, 4089; doi:10.3390/ma13184089

and 1100.607 mg/kg at 20°C for Mg-Al-LDHs (S1) and 407.5368 mg/kg at 10 °C and 436.9719 mg/kg at 20 °C for Mg-Ni-Al-LDHs (S2)) of adsorption capacity from Langmuir isotherm model. These obtained results shows that the adsorption of Mn^{2+} on Mg-Al-LDHs followed the Freundlich isotherm model which indicate that the adsorption belongs to multilayer. The comparisons of the maximum adsorption capacity among LDH and other related adsorbents are summarized in Table 2. The result demonstrated that the as-prepared Mg-Al-LDHs exhibited excellent removal capacity of Mn^{2+} than most of the adsorbents reported in literature [16-18]. Li *et al.* [16] synthesized Mn-doped MgAl-layered double hydroxides (LDHs) for removal arsenate from aqueous solution. The study indicated that the adsorption capacity of As(V) on Mn-LDHs via Langmuir isotherm model was 166.94 mg/g.

Bakr *et al.* [17] studied the removal of Mn(II) from aqueous solutions by Mg-Zn-Al LDH/montmorillonite nanocomposite. The results indicated that the maximum adsorption efficiency were 24.5, 26.4 and 28.9 mg/g at adsorbent mass of 0.25 g/L, initial Mn(II) concentration of 80 mg/L, pH of 6.0, stirring rate of 160 rpm, contact time of 75 min and temperatures 298, 308 and 318 K. The obtained results indicated that the increasing the temperature of the adsorption process increases the adsorption capacity due to the acceleration of some original slow adsorption steps [17, 18]. Also, can be due to the new adsorption active sites that being created on the adsorbent surface or could be due to the increases the solubility of the Mn(II) ions in the medium [19-22].

Table. 2. Summary of Mn^{2+} adsorption kinetics parameters by samples S1 and S2 at 10 °C and 20 °C

Temperature (°C)	Langmuir			Freundlich		
	K (mg^{-1}·L)	a_{max} (mg/kg)	R^2	K	m	R^2
		Sample S1				
10	0.04061	1048.32	0,97597	517.778	0.1948	0.9782
20	0.9529	1100.607	0.9586	635.637	0.1946	0.9808
		Sample S2				
10	0.2178	407.537	0.7282	169.095	0.2083	0.9096
20	0.1819	436.972	0.7568	155.57	0.2468	0.9206

As shown in the Table 2, all the used models correlated well with the experimental data (R^2 > 0.9) in the following order: Freundlich > Langmuir. The higher values of R^2 indicate that the Freundlich model was more suitable for describing the sorption equilibrium of manganese onto the LDH adsorbent. The manganese adsorption data obtained in this study were better represented by the Freundlich form than by the Langmuir form, as confirmed by the R^2 values, at temperature of 20 °C (Table 2). The Freundlich model provided the best fit to the data for the adsorption of Mn^{2+} onto Mg-Al-LDH (R^2 = 0.9808), indicating that the manganese monolayer adsorption on surface of the adsorbent was heterogeneous. This fact can be attributed to the incorporation of different elements from the wastewater into the Mg-Al-LDH structure during the synthesis procedure [19].

The calculated maximum Mn^{2+} adsorption capacity of 80.607 mg/kg was obtained for Mg-Al-LDH, indicating that mixed oxide LDH is a promising adsorbent that can be used in the removal of Mn^{2+} from wastewaters.

Peer-reviewed version available at Materials 2020, 13, 4089; doi:10.3390/ma13184089

3.2.1. Sorption kinetics

The experimental kinetic curves for Mn^{2+} sorption on Mg-Al-LDH and Mg-Ni-Al-LDH are presented in Figure 7.

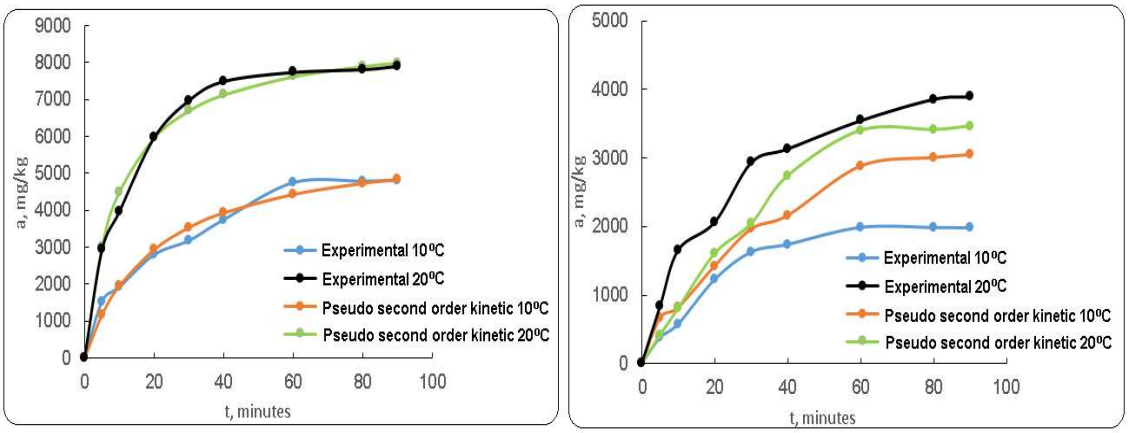

Figure 7. Integral kinetic curves for Mn^{2+} retention on Mg-Al-LDH and Mg-Ni-Al-LDH at 10 and 20°C

As can be seen, in all experiments the sorption reached equilibrium in approximately 60 minutes. The results are consistent with those derived from sorption isotherms (Figure 7).

Pseudo-first-order and pseudo-second-order were used to evaluate the kinetic sorption data. Linear forms of these kinetic models are presented in Equations (7)-(9) [17]. The kinetic parameters and the correlation coefficients are presented in Table 3.

$$\ln(q_e - q_t) = \ln q_e - k_1 t \quad (7)$$

$$\frac{t}{q_t} = \frac{1}{k_2 q_e^{\,2}} + \frac{t}{q_e} \quad (8)$$

$$q_t = K_{id} t^{1/2} + C \quad (9)$$

where q_e and q_t - in the above equations are the sorption capacity at equilibrium and at a time t, respectively, (g Mn^{2+}/g of sorbent), k_1 - the pseudo-first-order rate constant (min^{-1}), k_2 - the pseudo-second-order rate constant (g mg^{-1} min^{-1}), K_{id} - the diffusion rate coefficient (mg g^{-1} $min^{-1/2}$), C - the intercept and it is related to the thickness of the boundary layer.

According to the correlation coefficients (R^2) the kinetic sorption of Mn^{2+} was better evaluated by the pseudo-second-order kinetic model for all experiments. The kinetic rate (k_2) is always higher for Mg-Al-LDH (Table 3). These results are indicative for a higher affinity between Mn^{2+} and the available and well distributed active sorption sites of Mg-Al-LDH beads, which leads to a faster sorption. In addition, the sorption capacity of Mg-Al-LDH beads follows the same trend suggesting that the high surface area of Mg-Ni-Al-LDH.

Bakr *et al.* [18] applied the pseudo first order and pseudo second order models to evaluate the adsorption kinetics of Mn(II) ions onto Mg-Zn-Al LDH/montmorillonite nanocomposite. The results obtained indicated that by applying of the pseudo second order kinetic model the correlation coefficients were ranged between 0.996 and 0.999. That results validity the pseudo second order

Peer-reviewed version available at Materials 2020, 13, 4089; doi:10.3390/ma13184089

kinetic model to the adsorption data. Also the kinetic model revealed that the stage of determining the adsorption rate of Mn(II) metal ions was the chemical interaction between the metal ions and the adsorbent [23].

Table 3. Kinetic parameters and the correlation coefficients of Mn^{2+} sorption on Mg-Al-LDH (samples S1) and Mg-Ni-Al-LDH (sample S2), at 10°C and 20°C

Kinetic model	Parameters	Sample S1 10°C	Sample S2 10°C	Sample S1 20°C	Sample S2 20°C
Experimental	$q_{e,exp.}$	48.333	40.359	80.437	56.150
Pseudo-first order	$q_{e,calc.}$	97.055	63.471	76.524	38.164
	k_1, min^{-1}	0.132	0.155	0.143	0.147
	R^2	0.8832	0.9671	0.9623	0.8580
Pseudo-second order	$q_{e,calc.}$	50.000	56.250	93.093	49.020
	k_2, min^{-1}	0.0040	0.0045	0.0017	0.0012
	R^2	0.9917	0.9919	0.9958	0.9923

A higher sorption rate was observed at the initial reaction time when 80 mg/L of Mn^{2+} was employed. At 60 min of shaking time, 15%, and 95% of Mn^{2+} were removed for the initial concentration.

Yung *et al.* So studied the Adsorptive removal of phosphate by Mg-Al and Zn-Al layered double hydroxides. The results obtained indicated that the adsorption of phosphate onto Mg-Al and Zn-Al LDHs were governed by the pseudo-second-order kinetic model. This kinetic model indicates that the chemical adsorption or chemical bonding between adsorbent active sites and phosphate could dominate the adsorption process. The values of q_e for Mg–Al was 9.78 mg/g and fro Zn-Al LDHs was of 24.8 mg/g. These values indicated that the order for phosphate adsorption capacity was Zn-Al LDH >Mg-Al LDH [24].

3.3. Adsorption mechanisms

In general, three mechanisms have been proposed that control the elimination of contaminants using LDH, namely: surface adsorption, the anion exchange between layers, and reconstruction of calcined LDH precursors by memory effect [19]

Surface adsorption involves the attachment of contaminants to the surface of LDHs, thus allowing the formation of a molecule or a film.

The cationic exchange process of LDHs is mainly influenced by the load balancing anions in the intermediate layer, but also by the charge density of the layer. As a unit of construction, the double-lamellar hydroxides of Mg-Al-LDH and Mg-Al-Ni LDH type have the surface occupied with complete hydroxyl groups (OH-) or with deprotroned hydroxyl groups (-O-) which could form complexes with metal cations.

Peer-reviewed version available at Materials 2020, 13, 4089; doi:10.3390/ma13184089

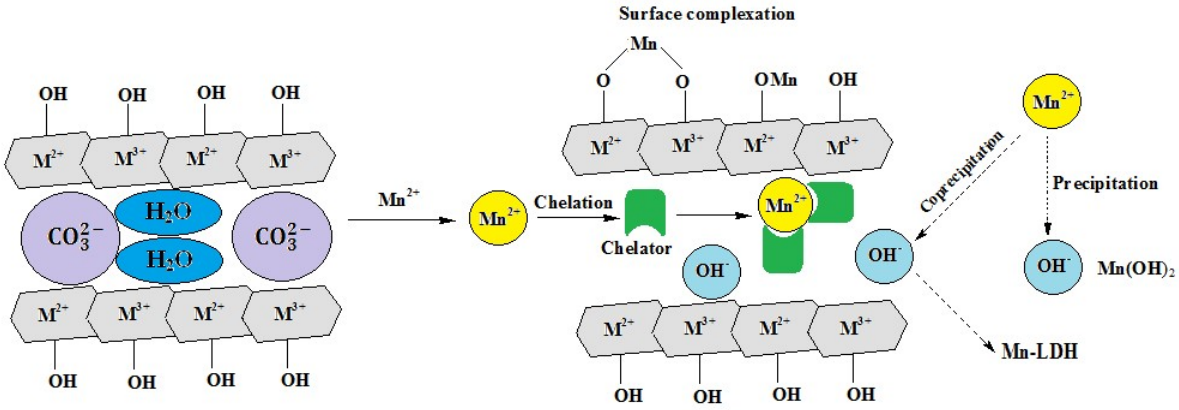

Figure 8. The possible adsorption mechanism of Mn^{2+}

According to the Pourbaix diagram, for manganese in aqueous solution, the Mn^{2+} species exist at pH values between 0 and 8.

So, it can be assumed that Mn^{2+} was removed mainly by the formation of surface complexes. However, the introduction of the Ni ion into the LDH structure could lead to an increase in pH due to the release of hydroxyl ions (OH-), and Mn^{2+} easily forms chemical precipitates which leads to a reduction in the adsorption capacity. The experimental results obtained suggested that the determining stage of speed may be chemical adsorption.

Therefore, the high adsorption capacity of Mn2+ on Mg-Al-LDH can be explained by the formation of four surfaces with loads between bivalent and trivalent cations, which means the formation of surface energy layers. In addition to the large surface area and the large exchange of anions, their flexible intermediate region, accessible to various molecular species, is another important feature that promises a high efficiency in removing contaminants (Figure 8).

4. Conclusions

The objective of this work was to synthetize, characterize and applied an Mg-Al and Mg-Ni-Al LDHs for removing Mn^{2+} from synthetical wastewaters similar to groundwater. The stirring time, pH effect, initial concentration of Mn^{2+} and competing ions, the adsorption kinetics and isotherms were also examined.

The success of the synthesis of the new material has been confirmed by XRD, SEM and EDX analysis that revealed new properties comparative with the basic material, namely brucite. The XRD patterns of LDHs before and after Mn^{2+} adsorption showed that the diffraction intensity of peaks decreases. This indicated that the manganese species was incorporated into the interlayer of the LDHs. The SEM image indicate that the LDH particles were uniformly shaped sheets, with most of them being hexagonal (gray parts). The prepared LDHs exhibit the agglomerates of compact and non-porous structure.

The adsorption of Mn^{2+} could reach equilibrium quickly at 60 min of shaking time. The pseudo-second-order expression accurately described the Mn^{2+} adsorption kinetics for the prepared LDHs. The adsorption capacity of Mn^{2+} increased with increasing the initial Mn^{2+} concentration. The calculated value was 1048.315 mg/kg at 10° C and 1100.607 mg/kg at 20°C for Mg-Al-LDHs and 407.5368 mg/kg at 10 °C and 436.9719 mg/kg at 20 °C for Mg-Ni-Al-LDHs of adsorption capacity from

Peer-reviewed version available at Materials 2020, 13, 4089; doi:10.3390/ma13184089

Langmuir isotherm model. The calculated maximum Mn^{2+} adsorption capacity of 80.607 mg/kg was obtained for (Mg-Al-Ni)-LDH. The adsorption experiments revealed that Mg-Al-LDH has a much higher adsorption capacity than Mg-Ni-Al-LDH for Mn^{2+}. Moreover, the high rate of adsorption of the three chemical species has been highlighted. In this regard, about 95% of them were removed from the aqueous solution in about 60 minutes.

The obtained results prove that the synthetized LDHs can be used as potential adsorbents for Mn^{2+} removal from wastewater.

Author Contributions: Conceptualization, C.M. and S.C.; Data curation, C.M., S.C. A.M.D. O.D.O and E.V; Formal analysis, C.M. and A.M.D.; Funding acquisition, O.D.O. and E.V.; Investigation, C.M., S.C. and A.M.D.; supervision: S.C. and A.M.D..; writing—original draft preparation, C.M., S.C. and A.M.D..; writing—review and editing, C.M., S.C. and A.M.D..; Software, E.V. All authors have read and agreed to the published version of the manuscript.

Acknowledgments: This work has been funded by University Politehnica of Bucharest, through the "Excellence Research Grants" Program, UPB – GEX 2017. Identifier: UPB- GEX2017, Ctr. No. 78/2017 Cod 136".

Conflicts of Interest: The authors declare no conflicts of interest

References

[1] Li, H.H.; Chen, L.J.; Yu, L.; Guo, Z.B.; Shan, C.Q.; Lin, J.Q.; Gu, Y.G.; Yang, Z.B.; Yang, Y.X.; Shao, J.R.; Zhu, X.M.; Cheng, Z. Pollution characteristics and risk assessment of human exposure to oral bioaccessibility of heavy metals via urban street dusts from different functional areas in Chengdu, China, *Science of The Total Environment* **2017,** *586*, 15, 1076-1084

[2] Levy, B.S. Nassetta, W.J. Neurologic Effects of Manganese in Humans: A Review, *Int J Occup Environ Health*, **2003**, *9*, 153-163

[3] Resolução CONAMA 430/2011, de 13 de Maio de 2011. Dispõem sobre as condições e padrões de lançamento de efluentes, complementa e altera a resolução nº357, de 17 de março de 2005, do Conselho Nacional do Meio Ambiente – CONAMA. Brasília, Ministério do Meio Ambiente, 2011.

[4] Silva, A.M.; Cunha, E.C.; Silva, F.D.R.; Leão, V.A. Treatment of high-manganese mine water with limestone and sodium carbonate. *Journal of Cleaner Production* **2012**, *29–30*, 11-19

[5] Zhang, W.; Cheng, C.Y.; Pranolo, Y.; Investigation of methods for removal and recovery of manganese in hydrometallurgical processes, *Hydrometallurgy* **2010**, *101*, 1–2, 58-63

[6] Aziz, H.A.; Smith, P.G. Removal of manganese from water using crushed dolomite filtration technique. *Water Research* **1996,** *30, 2*, 489-492

Peer-reviewed version available at Materials 2020, 13, 4089; doi:10.3390/ma13184089

[7] Han, M.; Zhao, Z.; Gao, W.; Cui, F. Study on the factors affecting simultaneous removal of ammonia and manganese by pilot-scale biological aerated filter (BAF) for drinking water pre-treatment. *Bioresource Technology* **2013**, *145*, 17-24

[8] Wimonsong, P.; Nitisoravut, R.; Llorca, J. Application of Fe–Zn–Mg–Al–O hydrotalcites supported Au as active nano-catalyst for fermentative hydrogen production. *Chemical Engineering Journal* **2014**, *253*, 1, 148-154

[9] Lin, J.; Jia, H.; Liang, H. ; Chen, S.; Cai, Y.; Qi, J. ; Qu, C. ; Cao, J. ; Fei, W.; Feng, J. Hierarchical $CuCo_2S_4$@NiMn-layered double hydroxide core-shell hybrid arrays as electrodes for supercapacitors. *Chemical Engineering Journal* **2018**, *336*, 15, 562-569

[10] Eisuke, T.K.; Yoshioka, K.T. Equilibrium and kinetics studies on As(V) and Sb(V) removal by Fe^{2+}-doped Mg–Al layered double hydroxides, *Journal of Environmental Management*, **2015**, *151*, 15, 303-309

[11] Sepehr, M.N.; Al-Musawi, T.J.; Ghahramani, E.; Kazemian, H.; Zarrabi, M, Adsorption performance of magnesium/aluminum layered double hydroxide nanoparticles for metronidazole from aqueous solution. *Arabian Journal of Chemistry* **2017**, *10*, 5, 611-623

[12] Birsanu, M.; Puscasu, M.; Gherasim, C.; Carja, G.; Highly efficient room temperature degradation of two industrial dyes using hydrotalcite-like anionic clays and their derived mixed oxides as photocatalysts, *Environmental Engineering and Management Journal* **2013**, *12*, 5, 1535 – 1540

[13] Gu, P.; Zhang, S.; Li, X.; Wang, X.; Wen, T.; Jehan, R.; Alsaedi, A.; Hayat, T.; Wang, X., Recent advances in layered double hydroxide-based nanomaterials for the removal of radionuclides from aqueous solution. *Environmental Pollution* **2018**, *240*, 493-505

[14] Cavani, F.; Trifirb, F.; Vaccari, A. Hydrotalcite-type anlonlc clays: preparation, properties and applications. *Catalysis Today* **1991**, *11*, 173-301

[15] Modrogan, C.; Orbuleț, O.D.; Orbeci, C.; Bobirică, C.; Dancila, A.M. Removal of manganese from groundwater by adsorption on gellan gum/Fe_3O_4 composite, *18th International Multidisciplinary Scientific Geoconferences SGEM 2018, Ecology, Economics, Eduction and Legislation Conference Proceedings* **2018**, 18(1), 705-711, ISI Proceedings; DOI: 10.5593/SGEM2018/5.1

[16] Li, S.; Guo, Y.; Xiao, M.; Zhang, T.; Yao, S.; Zang, S.; Fan, H.; Shen, Y.; Zhang, Z.; Li, W. Enhanced arsenate removal from aqueous solution by Mn-doped MgAl-layered double hydroxides. *Environ Sci Pollut Res Int* **2019**, *26(12)*, 12014-12024

[17] Bakr, A.A.; Sayed, N.A.; Salama, T.M.; Ali, I.O.; Abdel Gayed, R.R.; Negm, N.A. Kinetics and thermodynamics of Mn(II) removal from aqueous solutions onto Mg-Zn-Al LDH/montmorillonite nanocomposite. *Egyptian Journal of Petroleum* **2018**, *27*, 1215-1220

[18] Bakr, A.A.; Sayed, N.A.; Salama, T.M.; Ali, I.O.; Abdel Gayed, R.R.; Negm, N.A. Potential of Mg–Zn–Al layered double hydroxide (LDH)/montmorillonite nanocomposite in remediation of wastewater containing manganese ions. *Res. Chem. Intermed.* **2018**, *44*, 389–405

[19] Li, S.; Shen, Y.; Liu, D.; Fan, L.; Zhao, Y. Novel nanomaterials of 2-benzoylbenzoic acid anions intercalated magnesium aluminum layered double hydroxides for UV absorption properties. *Sci Adv Mater* **2015**, *7*, 756–761

[20] Teixeira, M.A.; Mageste, A.B.; Dias, A.; Virtuoso, L.S.; Siqueira, K.P.F. Layered double hydroxides for remediation of industrial wastewater containing manganese and fluoride. *Journal of Cleaner Production* **2018**, *171*, 275-284

Peer-reviewed version available at Materials 2020, 13, 4089; doi:10.3390/ma13184089

[21] Ai, L.; Zhang, C.; Chen, Z. Removal of methylene blue from aqueous solution by a solvothermal-synthesized graphene/magnetite composite. *Journal of Hazardous Materials* **2011**, *192(3)*, 1515–1524 doi:10.1016/j.jhazmat.2011.06.068

[22] Dho, N.Y.; Lee, S.R. Effect of Temperature on Single and Competitive Adsorptions of Cu(II) and Zn(II) Onto Natural Clays. *Environ. Monit. Assess.* **2003**, *83(2)*, 177-203

[23] Sadeek, S.A.; Negm, N.A.; Hefni, H.H.H.; Abdel Wahab, M.M. Metal adsorption by agricultural biosorbents: Adsorption isotherm, kinetic and biosorbents chemical structures. *Int. J. Biol. Macromol.* **2015**, *81*, 400–409

[24] Yang, K.; Yan, L.; Yang, Y.; Yu, S.; Shan, R.; Yu, H.; Zhu, B. B.D. Adsorptive removal of phosphate by Mg–Al and Zn–Al layered double hydroxides: Kinetics, isotherms and mechanisms. *Separation and Purification Technology* **2014**, *124*, 36–42